Vitamin D receptor–retinoid X receptor heterodimer signaling regulates oligodendrocyte progenitor cell differentiation

Alerie Guzman de la Fuente,[1] Oihana Errea,[1] Peter van Wijngaarden,[1,3] Ginez A. Gonzalez,[1] Christophe Kerninon,[2] Andrew A. Jarjour,[5] Hilary J. Lewis,[6] Clare A. Jones,[6] Brahim Nait-Oumesmar,[2] Chao Zhao,[1] Jeffrey K. Huang,[4] Charles ffrench-Constant,[5] and Robin J.M. Franklin[1]

[1]Wellcome Trust-Medical Research Council Stem Cell Institute, University of Cambridge, Cambridge CB2 0AH, England, UK
[2]Institut du Cerveau et de la Moelle Épinière, Institut National de la Santé et de la Recherche Médicale, Unité Mixte de Recherche 1127, 75651 Paris, France
[3]Centre for Eye Research, University of Melbourne, Royal Victorian Eye and Ear Hospital, Victoria 3002, Australia
[4]Department of Biology, Georgetown University, Washington, DC 20057
[5]Medical Research Council Centre for Regenerative Medicine, University of Edinburgh, Edinburgh EH16 4UU, Scotland, UK
[6]AstraZeneca, Great Abington CB21 6GH, England, UK

The mechanisms regulating differentiation of oligodendrocyte (OLG) progenitor cells (OPCs) into mature OLGs are key to understanding myelination and remyelination. Signaling via the retinoid X receptor γ (RXR-γ) has been shown to be a positive regulator of OPC differentiation. However, the nuclear receptor (NR) binding partner of RXR-γ has not been established. In this study we show that RXR-γ binds to several NRs in OPCs and OLGs, one of which is vitamin D receptor (VDR). Using pharmacological and knockdown approaches we show that RXR–VDR signaling induces OPC differentiation and that VDR agonist vitamin D enhances OPC differentiation. We also show expression of VDR in OLG lineage cells in multiple sclerosis. Our data reveal a role for vitamin D in the regenerative component of demyelinating disease and identify a new target for remyelination medicines.

Introduction

Remyelination involves the generation of new myelin sheath–forming oligodendrocytes (OLGs) after primary demyelination in the central nervous system (Franklin and Ffrench-Constant, 2008). OLGs are generated from multipotent progenitors referred to as OLG progenitor cells (OPCs), which, in response to demyelination, divide, migrate, and differentiate into mature OLGs (Levine and Reynolds, 1999; Zawadzka et al., 2010; Moyon et al., 2015). In common with other regenerative processes, remyelination efficiency declines with aging, with the result that in chronic demyelinating diseases such as multiple sclerosis (MS), remyelination becomes ineffective (Shields et al., 2000; Goldschmidt et al., 2009). Several lines of experimental evidence indicate impairment of OPC differentiation as the key determinant of the aging effects in remyelination (Wolswijk, 1998; Sim et al., 2002; Woodruff et al., 2004; Kuhlmann et al., 2008; Shen et al., 2008). Thus, the mechanisms regulating OPC differentiation are key to identifying targets for remyelination-enhancing therapy (Kotter et al., 2011).

We previously identified the nuclear receptor (NR) retinoid X receptor (RXR) γ as a positive regulator of OPC differentiation (Huang et al., 2011). The acceleration of remyelination in aged rodents after systemic delivery of an RXR-γ agonist identified RXR-γ as an attractive target for therapeutic remyelination, especially given the drug development activity around this NR in the context of other diseases (de Lera et al., 2007; Pérez et al., 2012). RXR-γ functions when bound to another NR as a heterodimer. Therefore, understanding which RXR-γ heterodimers are involved in the control of OPC differentiation is critically important for fully exploiting the therapeutic potential of RXR signaling.

Results and discussion

RXR-γ–vitamin D receptor (VDR) complex in OLG lineage cells

RXR-γ binding partners were identified using whole cell lysates obtained from cultures of OPCs or OLGs. OPCs isolated from a mixed glial culture (MGC) were maintained in the presence of PDGF-AA and basic FGF (bFGF). OLGs were generated
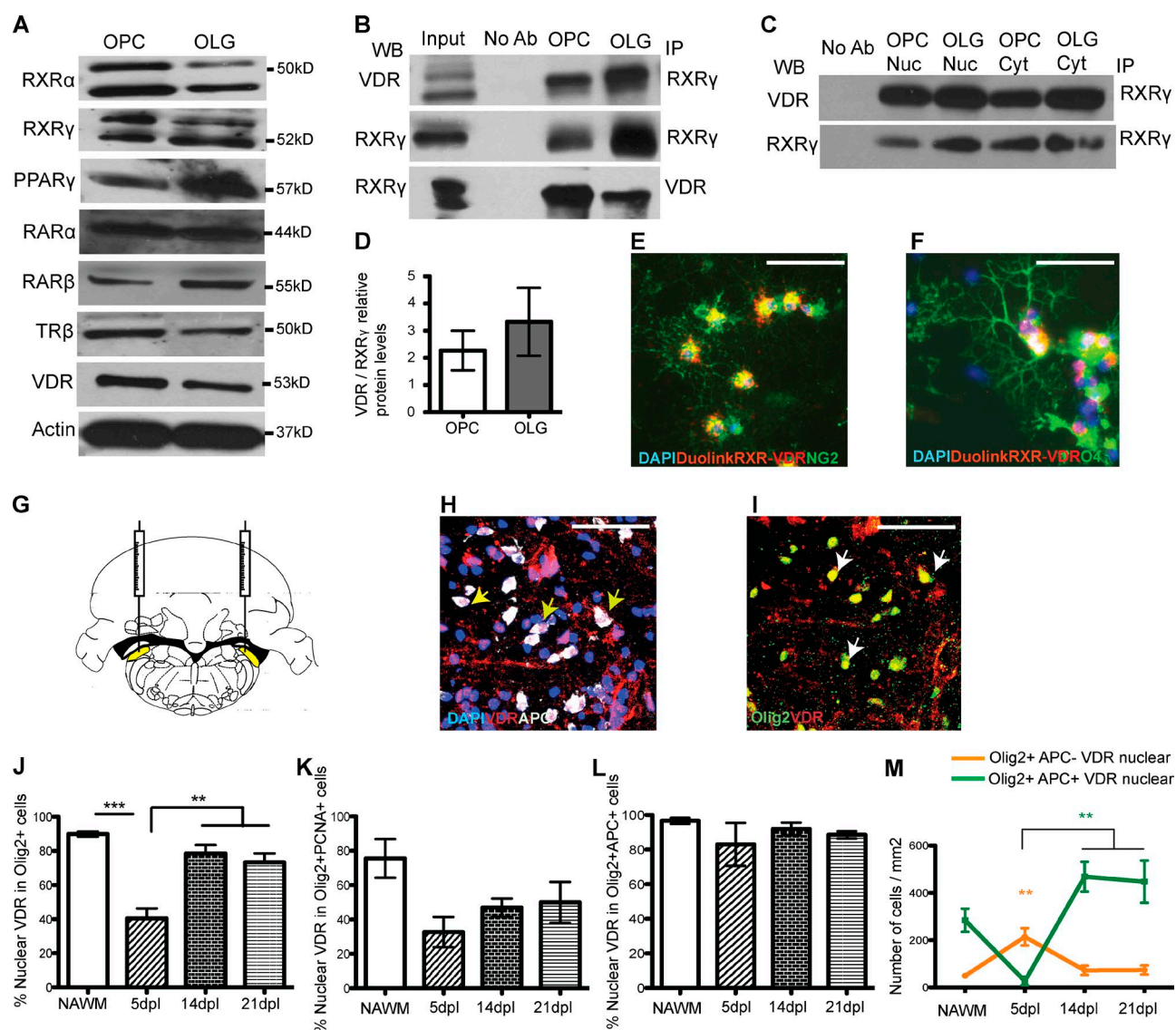
Figure 1. **The NR VDR is expressed and bound to RXR-γ in OLG lineage cells.** (A) Western blot showing expression of NRs in OPCs and OLGs. (B) CoIP showing binding between VDR and RXR-γ. (C) CoIP of subcellular fractions showing VDR and RXR-γ complexes in the nucleus and cytoplasm of OPCs and OLGs. (D) Quantification shows no difference in VDR–RXR-γ binding in OPCs and OLGs (n = 3; unpaired Student's t test). (E and F) Duolink immunostaining showing VDR–RXR-γ binding (red) in OPCs stained for NG2 (E) and O4 (F). (G) Ethidium bromide is injected into the rat CCP to induce focal demyelination. (H and I) Immunostaining of a 21-dpl CCP lesion showing colocalization of APC–VDR (H; yellow arrows) and VDR–Olig2 (I; white arrows). (J) The proportion of Olig2+ cells expressing VDR in the nucleus increases at 14 and 21 dpl and is similar to NAWM (n = 4; one-way ANOVA and Bonferroni post-hoc test). (K) The proportion of Olig2+PCNA+ cells expressing VDR does not change with the lesion. (L) The proportion of Olig2+APC+ cells expressing nuclear VDR does not vary after lesioning. (K and L) n = 4; one-way ANOVA. (M) Density of OPCs (APC−, yellow) and OLGs (APC+, green) with nuclear VDR expression during remyelination (n = 4; one-way ANOVA and Bonferroni post-hoc test). Bars, 50 µm. Mean ± SEM. **, P < 0.01; ***, P < 0.001.

by growing OPCs in medium without these two growth factors for 5 d in vitro (DIV). RXRs α and γ, retinoid acid receptors (RARs) α and β, VDR, thyroid hormone receptor β, and peroxisome proliferator activated receptor (PPAR) γ were detected in OPCs and OLGs (Fig. 1 A).

To identify the NRs bound to RXR-γ within OLG lineage cells, we performed coimmunoprecipitation (CoIP) assays. VDR, together with RAR-β and PPAR-γ (unpublished data), were pulled down with RXR-γ in OPC and OLG lysates (Fig. 1, B and D). Because of the association of hypovitaminosis D and MS, we focused on VDR (Ascherio et al., 2012; Burton and Costello, 2015). CoIP assays revealed no differences in RXR-γ–VDR binding in nuclear and cytoplasmic fractions from either OPCs or OLGs (Fig. 1 C). Using a

proximity ligand assay (PLA; Duolink), which enables protein binding to be visualized in cells, we detected binding of VDR to RXR-γ in NG2+ OPCs (Fig. 1 E) and O4+ OLG lineage cells (Fig. 1 F).

To determine VDR expression in OLG lineage cells during remyelination, we induced focal demyelination by injecting ethidium bromide into the caudal cerebellar peduncle (CCP) of 2-mo-old rats (Fig. 1 G; Woodruff and Franklin, 1999). We used antibodies to adenomatous polyposis coli (APC; a marker of mature OLGs), Olig2 (an OLG lineage marker), and VDR to analyze VDR cellular localization in normal-appearing white matter (NAWM) and at 5 d post lesion (dpl), when OPC recruitment is maximal, at 14 dpl, when recruited OPCs are undergoing differentiation and new myelin sheaths appear, and at

21 dpl, when remyelination is complete. APC$^+$ and Olig2$^+$ cells both expressed nuclear VDR (Fig. 1, H and I). The proportion of Olig2$^+$ cells expressing nuclear VDR was decreased at 5 dpl compared with NAWM, but at 14 and 21 dpl, there were no differences with NAWM (Fig. 1 J). Olig2$^+$ cells that did not express APC were taken to be OPCs and immature OLGs. At 5 dpl, there was a significant increase in the density of Olig2$^+$/APC$^-$ cells with nuclear VDR expression, indicating a high level of VDR expression in activated recruited OPCs. As the number of OPCs declined at 14 and 21 dpl, there was a corresponding increase in the number of APC$^+$ cells expressing VDR (Fig. 1 M). The majority of APC$^+$ cells (∼90%) expressed nuclear VDR expression at all the time points and in NAWM (Fig. 1 L).

Blocking VDR signaling impairs OPC differentiation

To test the role of VDR signaling in the OLG lineage, we suppressed VDR activity in OPCs using ZK159222, a synthetic VDR antagonist. ZK159222 binds to VDR with less affinity than vitamin D and prevents binding of coactivators such as SRC1, preventing transcription of target genes (Herdick et al., 2000; Schmitz et al., 2015). The cells were then characterized using antibodies to Olig2 and Ki67 to study the effect of ZK159222 on the OPC cell cycle (Fig. 2 A). After 24 h of exposure to ZK159222, there was a twofold increase in the proportion of Olig2$^+$ cells expressing Ki67 (Fig. 2 B). We next asked whether the increase in proliferation was associated with impaired OPC differentiation because there is a mutual exclusivity between OPC proliferation and differentiation (Casaccia-Bonnefil and Liu, 2003). To address this, we cultured OPCs in medium without PDGF-AA and bFGF and exposed them to ZK159222. We then stained for Olig2 and myelin basic protein (MBP), a protein expressed by mature OLGs (Fig. 2 C). After a 24-h treatment with 0.2-μM ZK159222, we observed a 47.6% decrease in the proportion of MBP$^+$ cells within the Olig2$^+$ population compared with controls (Fig. 2 D), whereas 0.5-μM ZK159222 decreased levels by 31.0% (Fig. 2, E and F). Cell death was assessed by propidium iodide staining and showed no differences between control and ZK159222 treatment (Fig. 2 G).

To validate these data, we transfected OPCs with siRNA against VDR and a control nontargeting siRNA. Western blotting showed that transfection with VDR siRNA caused a significant decrease in VDR protein levels compared with the control (Fig. 2 J). After transfection with VDR siRNA, the proportion of Olig2$^+$ cells expressing MBP decreased to 63.4% of that in cells transfected with control siRNA, whereas the proportion of cells expressing Ki67 increased by 80.4% (Fig. 2, H, I, and K). Transfection did not affect cell death (Fig. 2 L). Thus, blocking VDR impaired OPC differentiation while increasing proliferation.

RXR agonists promote OPC differentiation via VDR heterodimers

Because 9-*cis*-retinoic acid (9cRA), an RXR agonist, enhances OPC differentiation (Huang et al., 2011), we next asked which component of the RXR-γ–VDR heterodimer was dominant. When OPCs in differentiation medium were treated with the VDR antagonist ZK159222 together with 9cRA, the proportion of MBP$^+$ cells decreased by 51.60% when compared with 9cRA treatment alone (Fig. S1 A). Thus, blocking signaling via VDR affects RXR signaling, and VDR needs be activated for 9cRA to exert its prodifferentiating effect.

Vitamin D increases OPC differentiation through VDR signaling

We next tested activation of VDR with vitamin D. We treated OPCs for 24 h with vitamin D (1,25-dihydroxyvitamin D3 or calcitriol) and examined proliferation and differentiation using antibodies to Ki67, MBP, and Olig2. Compared with untreated cultures, there was no difference in OPC survival, proliferation, and differentiation or in Olig2 expression (Fig. S2, A–F). Treatment with vitamin D and 9cRA had no additional effect compared with 9cRA treatment alone (Fig. S2, G and H).

We hypothesized that the lack of effect of vitamin D was caused by the presence of saturating concentrations of vitamin D in the culture media resulting from the exposure of OPCs to FBS (which contains traces of steroidal molecules including vitamin D) before isolation from MGCs. To test this, FBS was treated with activated charcoal to remove steroids by adsorption before its addition to the MGC media. We then exposed OPCs grown in charcoal-stripped serum to vitamin D for 24 h. Treatment with 0.1-μM vitamin D increased the number of Olig2$^+$ cells expressing MBP by 80.1% (Fig. 3, A and B) and decreased the number of Olig2$^+$ cells expressing Ki67 by 47.0% (Fig. 3, E and F) without affecting Olig2 expression (Fig. 3 H). MBP protein levels increased by 58.8% after vitamin D treatment (Fig. 3, C and D), and there was no difference in cell survival (Fig. 3 G).

To determine whether the vitamin D effects on OPCs were mediated via VDR, we treated OPCs with vitamin D and the VDR antagonist ZK159222 simultaneously. Vitamin D addition canceled the effect of ZK159222 on proliferation in OPCs derived from MGCs cultured with conventional serum (Fig. 3 I), whereas ZK159222 canceled the effect of vitamin D on differentiation in OPCs derived from MGCs cultured with charcoal-stripped serum (Fig. 3 J). These data indicate that vitamin D enhances OPC differentiation at the expense of OPC proliferation through VDR activation. 9cRA alone did not increase OPC differentiation in charcoal-stripped serum, supporting a key role for VDR in the prodifferentiating effect of 9cRA (Fig. S1 B).

Blocking VDR impairs myelination and remyelination

We next tested the effects of the VDR antagonist in an ex vivo cerebellar slice model of toxin-induced demyelination and remyelination. Cerebellar slices, cultured for 7 d before the addition of the VDR antagonist, were stained for MBP and neurofilament H (NFH), an axonal marker (Fig. 4 A), to assess myelination. Exposure to 0.2-μM ZK159222 decreased myelination by 37%, whereas 2-μM ZK159222 decreased myelination by 52% when compared with controls (Fig. 4 B). We then tested the effects of the VDR antagonist on remyelination. After 7 d in culture, slices were demyelinated with lysolecithin (Birgbauer et al., 2004). The lysolecithin-containing medium was then replaced with normal medium with 1% DMSO as the vehicle control, or with 0.2-μM or 2-μM ZK159222 (Fig. 4 C). We quantified remyelination as the area of MBP and NFH colocalization normalized to the total area of NFH staining. At 6 dpl, only 2-μM ZK159222 caused a decrease in remyelination compared with controls, whereas at 8 dpl, 0.2-μM ZK159222 and 2-μM ZK159222 had 42% and 48% less remyelination, respectively (Fig. 4 D). Thus, VDR activation plays a role in both myelination and remyelination.
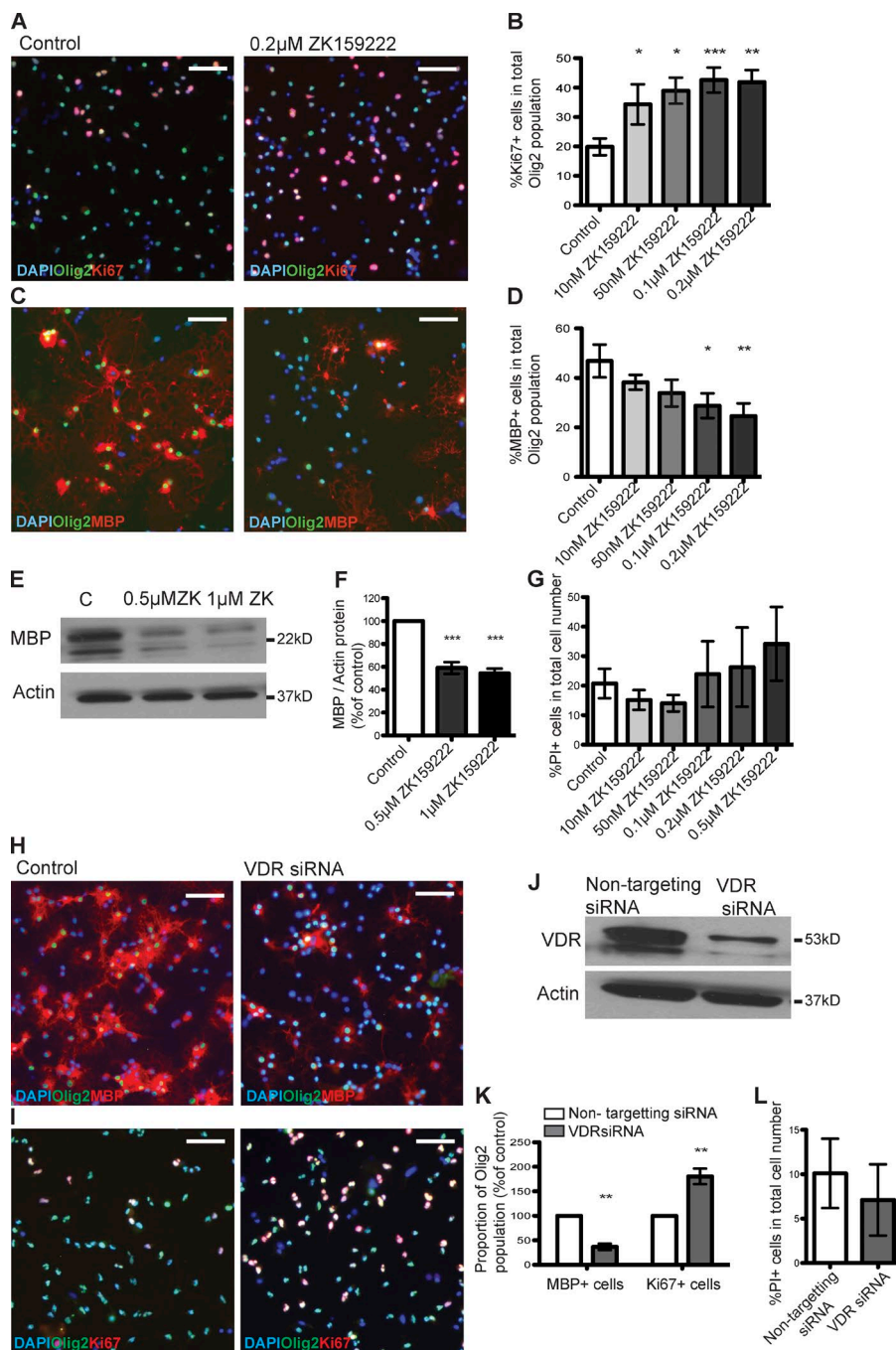
Figure 2. **The blocking of VDR impairs OPC differentiation.** (A) OPCs treated with vehicle or 0.2-µM ZK159222 stained with antibodies against Ki67 and Olig2. (B) Treatment with ZK15922 increases OPC proliferation. (C) OPCs treated with vehicle or 0.2µM ZK159222 stained for MBP and Olig2. (D) Treatment with ZK159222 impairs OPC differentiation. (B and C) $n = 5$; one-way ANOVA and Dunnett's post-hoc test. (E and F) Treatment with ZK159222 for 48 h decreases MBP protein levels when compared to control ($n = 3$; one-way ANOVA and Dunnett's post-hoc test). (G) Treatment with ZK159222 does not affect cell death ($n = 4$; one-way ANOVA). (H and I) OPCs treated with nontargeting siRNA or VDR siRNA for 48 h and stained with antibodies against MBP (H) and Ki67 (I). (J) Western blot showing VDR protein levels 48 h after siRNA treatment. (K and L) VDR siRNA impairs OPC differentiation (K) and increases OPC proliferation (L; $n = 4$; unpaired Student's t test). Bars, 50 µm. Mean ± SEM are shown. *, $P < 0.05$; **, $P < 0.01$; ***, $P < 0.001$. C, control; PI, propidium iodide.

VDR is highly expressed in active MS plaques

To assess the relevance of these findings to human disease, we examined the expression of VDR in lesions from individuals with MS. Lesions were classified as periplaque white matter (PPWM), active lesions with remyelination capacity, and chronic lesions with either impaired or complete remyelination (Lucchinetti et al., 2000). Immunostaining was performed on snap-frozen postmortem brain sections obtained from randomly chosen individuals with MS and equivalent controls using an antibody against VDR together with antibodies that stain for the major central nervous system cell types. VDR was expressed in every cell type examined, including Sox10^{+} and Olig1^{+} OLG lineage cells (Fig. 5, A and B), major histocompatibility complex class II (MHC-II)–expressing microglia/macrophages (Fig. 5 C), myelin OLG glycoprotein (MOG)–expressing OLGs (Fig. 5 D), NeuN^{+} neurons (Fig. 5 E), and glial fibrillary acidic protein (GFAP)–expressing astrocytes (Fig. 5 F). The density of VDR-expressing cells in lesion tissue was compared with that of comparable NAWM regions in control subjects without MS. Active lesions contained a 3.6-fold increase in VDR[+] cell density when compared with NAWM controls and a 1.3-fold increase when compared with PPWM. Chronic lesions had 71.1% fewer VDR-expressing cells than active lesions. The only remyelinated lesion identified was full of VDR-expressing cells (Fig. 5 J). The density of cells with nuclear VDR localization was 74.7% higher in active lesions than in chronic lesions, 60.2% higher than in PPWM, and 81.5%
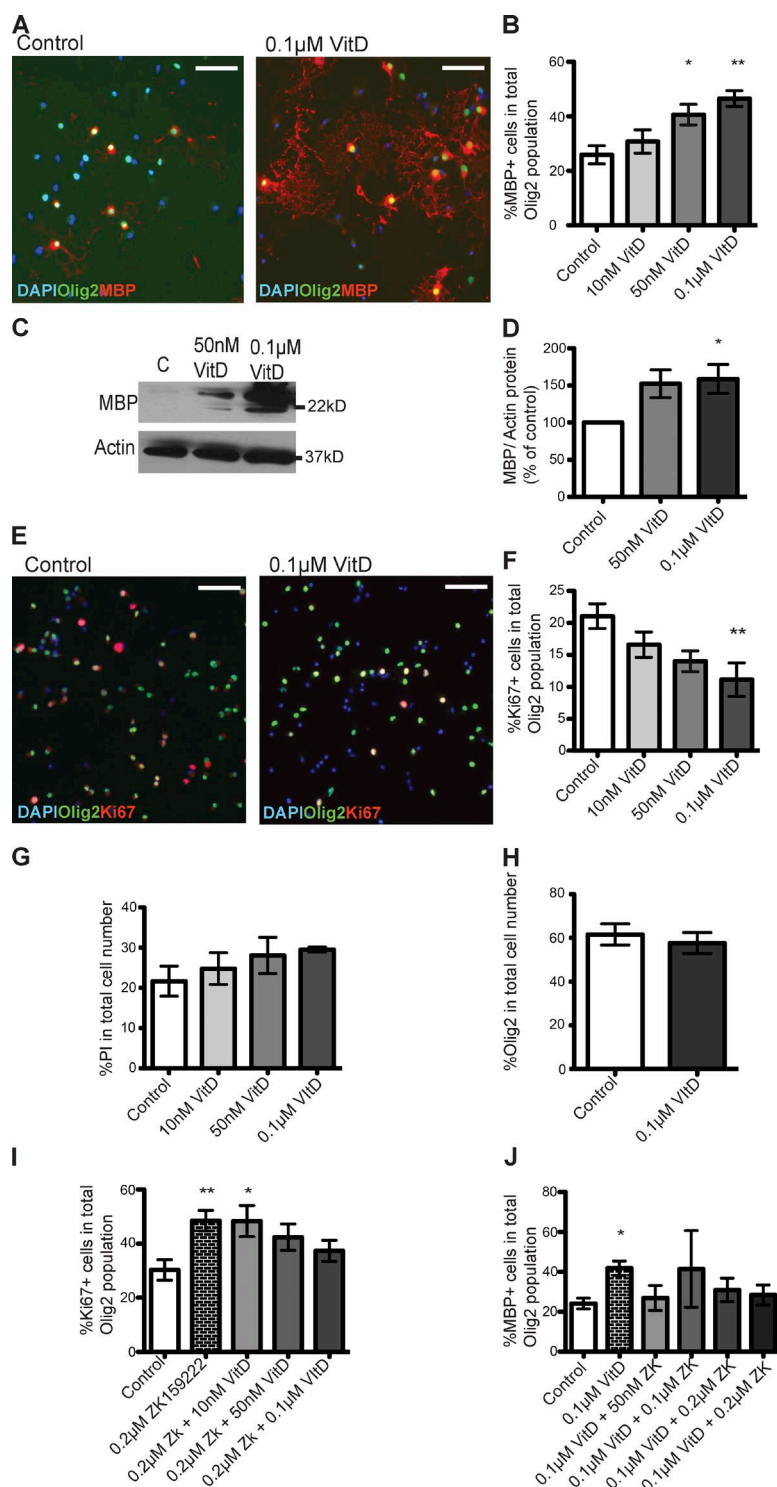
Figure 3. **Vitamin D treatment enhances OPC differentiation and decreases proliferation.** (A) OPCs treated with vehicle or 0.1-µM vitamin D and stained for MBP and Olig2. (B) Vitamin D increases OPC differentiation (*n* = 4). (C and D) Western blot (C) and quantification (D) demonstrating increased MBP after 48 h of vitamin D treatment. (n = 5; one-way ANO VA, Dunnett's post-hoc test. (E) Vehicle and 0.1-µM vitamin D–treated OPCs stained for Ki67 and Olig2. (F) Treatment with vitamin D decreases the number of proliferating Olig2^{+} cells (*n* = 6). (G and H) Vitamin D treatment does not alter OPC cell death (G; *n* = 2; one-way ANOVA) or Olig2 expression (H). (I and J) Treatment with vitamin D and ZK159222 in OPCs derived from MGCs exposed to control (I; *n* = 7) and charcoal-stripped serum (J; *n* = 3; one-way ANOVA and Dunnett's post-hoc test) show that they abrogate each other's effect. (B–D, F, I, and J) One-way ANOVA and Dunnett's post-hoc test were used. Bars, 50 µm. Mean ± SEM are shown. *, P < 0.05; **, P < 0.01. PI, propidium iodide.

higher than in NAWM controls, whereas no differences in cytoplasmic VDR were detected (Fig. 5 J). Within active lesions, 30.2% of VDR^{+} cells were also Sox10^{+} OLG lineage cells, whereas the remaining cells were mainly GFAP[+] astrocytes or MHC-II[+] monocytes/macrophages. This expression pattern, resembling that of RXR-γ (Huang et al., 2011), suggests a role for VDR in regeneration of MS lesions.

Here, we identify vitamin D and its cognate NR VDR as a positive regulator of OPC differentiation. Although VDR expression has previously been reported in cultured OPCs

and in human MS tissue (Baas et al., 2000; Eyles et al., 2005; Smolders et al., 2013), this study reveals that in OLG lineage cells VDR heterodimerizes with RXR-γ, a determinant of OPC differentiation (Huang et al., 2011), and is expressed in OPCs during remyelination (Fig. 1). Using pharmacological and knockdown approaches, we show that blocking VDR impairs OPC differentiation in vitro and during myelination and remyelination (Figs. 2 and 4; Birgbauer et al., 2004; Zhang et al., 2011; Jarjour et al., 2012). Moreover, activating VDR via vitamin D increases OPC differentiation (Fig. 3) in line
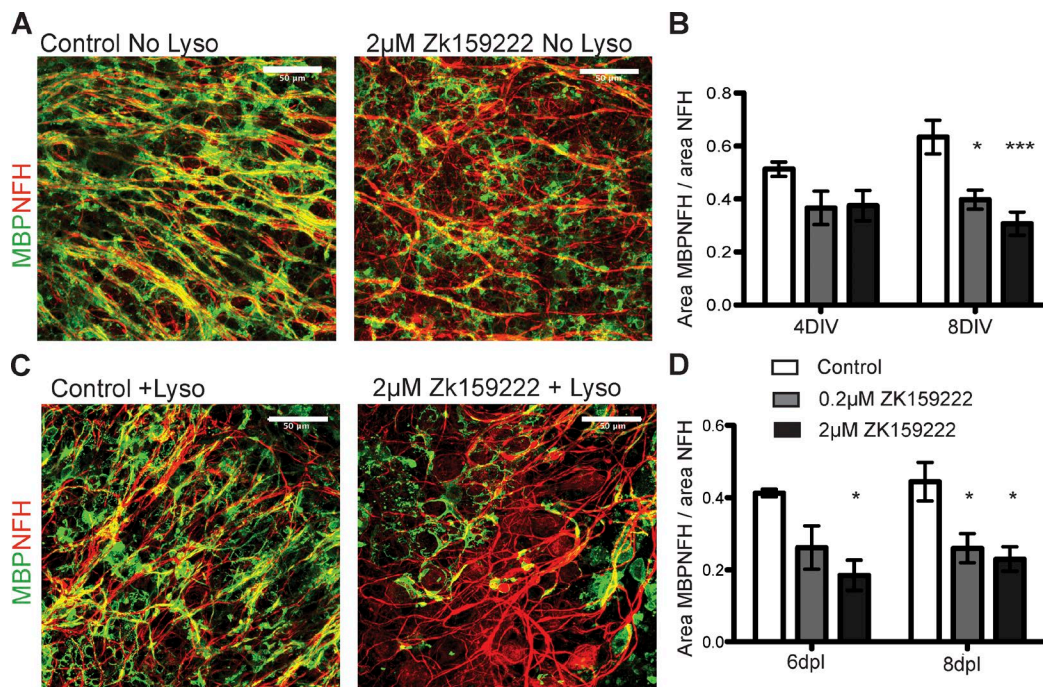
Figure 4. **VDR antagonist ZK159222 impairs myelination and remyelination in cerebellar slices.** (A) Cerebellar slices were exposed to the vehicle or 2-µM ZK159222 for 8 DIV. Staining shows MBP (green) and NFH (red). (B) Treatment with 0.2-µM and 2-µM ZK159222 impairs myelination ($n = 5$; one-way ANOVA and Dunnett's post-hoc test). (C) Cerebellar slices were demyelinated with lysolecithin (Lyso) and exposed to vehicle (DMSO) and ZK159222 for 8 d. (D) Exposure to 0.2-µM and 2-µM ZK159222 after demyelination impairs remyelination in a dose-dependent manner ($n = 3$; two-way ANOVA and Dunnett's post-hoc test). Bars, 50 µm. Mean ± SEM are shown. *, $P < 0.05$; ***, $P < 0.001$.

with a recent study demonstrating enhanced differentiation of neural stem cells toward the OLG lineage by vitamin D (Shirazi et al., 2015).

Epidemiological data have established an indirect link between the risk of developing MS and vitamin D deficiency (McLeod and Cooke, 1989; Munger et al., 2004, 2006; Soilu-Hänninen et al., 2005, 2008; Ascherio, 2013; Mokry et al., 2015). Thus far, the focus has been on the protective and immunomodulatory role of vitamin D in experimental autoimmune encephalomyelitis, an animal model for MS (Lemire and Archer, 1991; Cantorna et al., 1996; Nataf et al., 1996; Garcion et al., 2003). Our data suggest that hypovitaminosis D in MS patients may be a contributor to remyelination failure.

Previous studies have indicated a role for vitamin D in myelination and remyelination (Goudarzvand et al., 2010; Wergeland et al., 2011; Chabas et al., 2013; Nystad et al., 2014; Montava et al., 2015). These data, together with ours, highlight its potential for remyelination therapies. VDR is also expressed in microglia/macrophages (Fig. 5; Zhang et al., 2014). Because vitamin D decreases inducible nitric oxide synthase expression in microglia (Garcion et al., 1998), it may be one of the mechanisms that shifts the balance between pro- and antiinflammatory states known to be important for controlling remyelination (Miron et al., 2013). Vitamin D also increases microglial activation (Nystad et al., 2014) and amyloid-β phagocytosis (Masoumi et al., 2009), suggesting that it may also facilitate myelin debris clearance and thus remyelination (Kotter et al., 2006). Further investigation into the molecular mechanisms of VDR in remyelination will open up new opportunities for the development of regenerative medicines for demyelinating diseases.
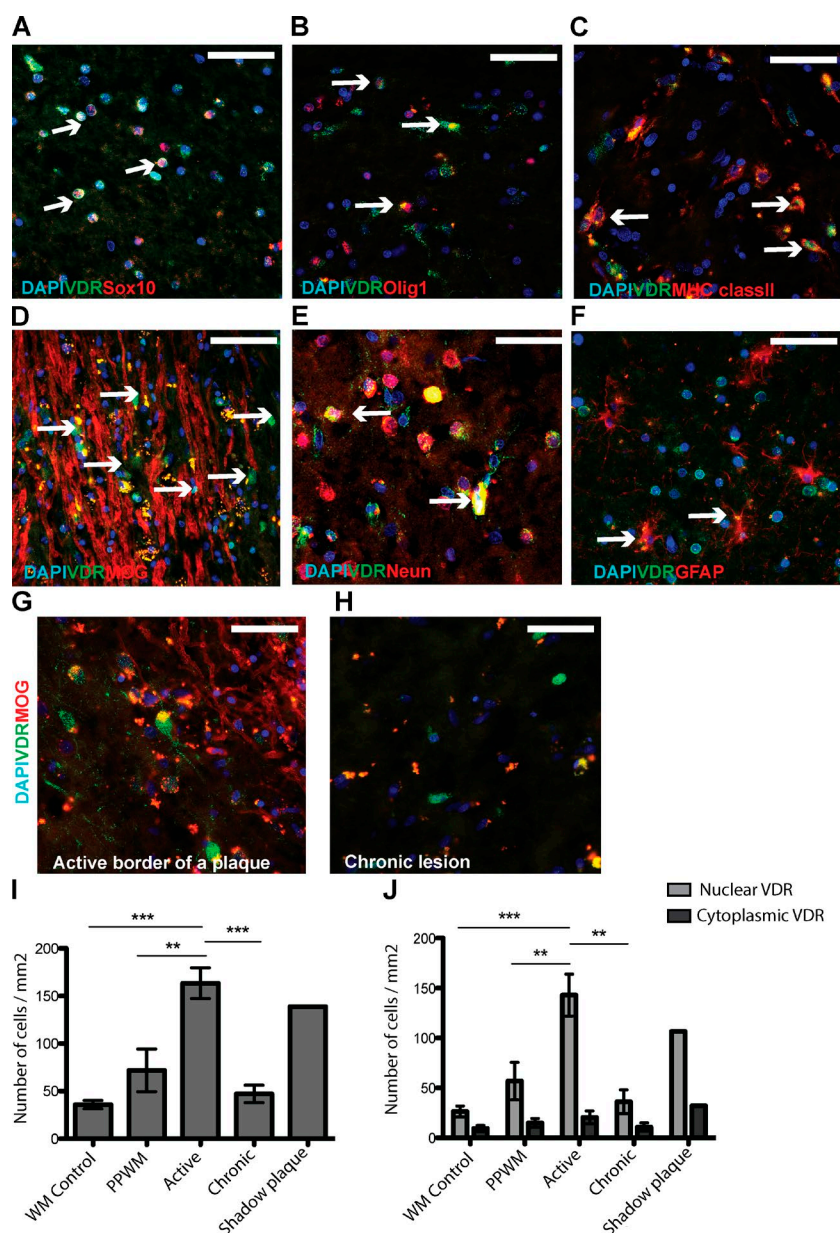
Materials and methods

OPC culture

OPC cultures were prepared from neonatal (postnatal day [P] 0–2) Sprague-Dawley rats as described previously (McCarthy and de Vellis, 1980). MGCs were kept for 11 DIV in DMEM (Gibco), 10% FBS (Biosera), and Mycozap PR-Plus (Lonza) before OPC selection. OPCs were isolated by shaking off nonadherent or loosely adherent cells (rich in OPCs) from the underlying adherent cell monolayer. Upon isolation, a relatively pure population of OPCs (71% Olig2^{+} [OLG lineage marker], 16% cell death [generally OPCs], 7% GFAP^{+} [astrocytes], and 5% CD11b^{+} cells [microglia]) were seeded onto poly-D-lysine–coated (Sigma-Aldrich) 13-mm coverslips for immunostaining, or T25 cell culture flasks for immunoprecipitation and Western blotting. Isolated OPCs were cultured at 37°C in 5% CO_2 in SATO medium (DMEM [Gibco], 1% penicillin/streptomycin, 10 µg/ml BSA, 0.06 µg/ml progesterone, 16.10 µg/ml putrescine, 0.005 µg/ml sodium selenite, 5 µg/ml insulin, and 50 µg/ml holotransferrin [Sigma-Aldrich]). A high proportion of OPCs within the cell culture was maintained by daily addition of 10 ng/ml PDGF-AA and 10 ng/ml bFGF (PeproTech). OLG-rich cultures were obtained by culturing OPCs in SATO media without growth factors. For both OPC and OLG cultures, thyroxine and thiiodothyronine were absent from the culture media. For differentiation experiments, OPCs were cultured in the presence of DMSO (Sigma-Aldrich), ZK159222, vitamin D (Sigma-Aldrich), or the corresponding combinations in the indicated concentrations 1 d after OPC isolation for another 24 or 48 h. ZK159222 was provided by E. May and A. Steinmeyer (Bayer Pharma AG, Berlin, Germany).

Serum charcoal stripping

For charcoal treatment, FBS was incubated with 2.5% (wt/vol) activated charcoal (Sigma-Aldrich) for 18 h at 4°C and filtered before

Figure 5. **VDR expression in brain lesions from humans with MS.** (A–F) Immunostaining with antibodies against VDR and Sox10 (A), Olig1 (B), MHC-II (C), MOG (D), NeuN (E), and GFAP (F). Arrows indicate double-positive cells. (G and H) Immunostaining with VDR and MOG shows nuclear localization and higher expression in the plaque border (G) and near absence in a chronic lesion (H). (I) VDR is highly expressed in active plaques and remyelinated plaques. (J) Nuclear VDR is expressed in active and remyelinated lesions to a greater extent than in chronic nonremyelinated lesions and white matter (WM) control, and cytoplasmic VDR density is similar for all lesion types. (I and J) $n = 5$; one-way ANOVA and Bonferroni post-hoc test. Mean ± SEM are shown. **, $P < 0.01$; ***, $P < 0.001$. Bars, 50 µm.

adding it to the MGC medium. Depletion of vitamin D was verified by mass spectrometry using previously described methods (Table S2; Bruce et al., 2013; van den Ouweland et al., 2014). In brief, a standard calibration curve was generated by spiking vitamin D into horse serum previously determined to give no signal. 150 µl of 0.2-M ZnSo$_4$ was added to each sample followed by vortexing for 1 min. 600 µl methanol was then added with vortexing for a further 5 min. The precipitate was sedimented by centrifugation. A solid phase extraction plate (Oasis HLB µElution; Waters) was conditioned with 200 µl methanol followed by 60% (vol/vol) methanol. 600 µl of each supernatant from sample pretreatment was loaded followed by two wash steps: 200 µl of 5% (vol/vol) methanol and then 200 µl of 60% (vol/vol) methanol. Retained analytes were eluted and transferred to amber glass vials before liquid chromatography (LC)–mass spectrometry analysis. The LC–mass spectrometry/mass spectrometry system was comprised of an ultra-performance LC system (Acquity I-Class; Waters) coupled to a triple quadrupole mass spectrometer (Xevo TQ-S; Waters) operating in positive electrospray ionization mode and using MassLynx software version 4.1 (Waters). 20 µl of

each sample was injected into a 2.1 × 50-mm ultra-performance LC ethylene-bridged hybrid phenyl column (Acquity; Waters) with 1.7 µl maintained at 35°C. The data were independently verified by SAS Bone Metabolic Laboratories.

CoIP

CoIP was performed according to the instructions on the cross-linking CoIP kit (Thermo Fisher Scientific). In brief, OPCs and OLGs were grown for 5 DIV and lysed with immunoprecipitation lysis wash buffer (0.025-M Tris, 0.15-M NaCl, 0.001-M EDTA, 1% NP-40, and 5% glycerol; Thermo Fisher Scientific) with Halt protease and phosphatase inhibitor cocktail (Thermo Fisher Scientific). Protein concentration was measured by bicinchoninic acid assay (Thermo Fisher Scientific), and immunoprecipitation was performed following the Pierce cross-link immunoprecipitation kit protocol (Thermo Fisher Scientific). In brief, 10 µg RXR-γ antibodies (ab15518; Abcam) were bound to protein A–coated agarose beads. Between 200 and 600 µg of protein were incubated overnight at 4°C with the antibody. Elution was analyzed by Western blotting.

Western blotting

Protein lysate was mixed with NuPAGE loading buffer and NuPAGE reducing agent (Invitrogen) and boiled for 10 min at 95°C. 5–15 µg of protein (lysed as described in the CoIP section) or total CoIP elution was loaded in 4–12% Bis-Tris gels (NuPAGE Novex; Invitrogen). After, electrophoresis gels were transferred to nitrocellulose membranes (GE Healthcare) and blocked with 5% milk in 0.1% PBS with Tween 20 (PBST). Membranes were incubated overnight at 4°C with the previously mentioned antibodies diluted in 5% nonfat dry milk in PBST. Upon three PBST washes, membranes were incubated with peroxidase-conjugated secondary antibodies (Dako) for 2 h at 20–26°C and developed with ECL (GE Healthcare) or Supersignal (Thermo Fisher Scientific) depending on the antibody. Western blot analysis was performed measuring the integrated density of the corresponding bands and normalizing them to β-actin (Sigma-Aldrich) control or CoIP control antibody, which is an antibody against the protein for which the pull-down has been done (RXR-γ in most cases).

Duolink

After fixation in 4% PFA, cells were stained using the Duolink in situ CoIP protocol (Olink; Sigma-Aldrich). Cells were blocked with Olink blocking solution for 1 h at 20–26°C. Primary antibodies against NRs were diluted in antibody diluent solution and incubated for 1 h at 20–26°C. PLA probe minus and PLA probe plus conjugated secondary antibodies were added and incubated for 1 h at 37°C. Next, PLA probes for the secondary antibodies were ligated by a 30-min incubation at 37°C with ligation solution, and the DNA signal was amplified by incubating the cells for 100 min at 37°C with DNA polymerase and fluorescent deoxynucleotide solution. OLG lineage marker antibodies were then added following the usual immunocytochemistry protocol.

siRNA transfection

After shake off, OPCs were kept for 2 DIV with growth factors, and then the medium was changed to SATO medium without penicillin/streptomycin overnight. Cells were transfected with 50-nM siRNA for VDR or for nontargeting control (GE Healthcare) using 1% Lipofectamine siRNAMAX (Invitrogen) diluted in Opti-MEM (Gibco) according to the manufacturer's protocol. After 6 h of transfection, the medium was replaced by normal SATO medium, with or without growth factors and without thyroxine or triiodothyronine. After 48 h of transfection, cells on coverslips were fixed with 4% PFA or lysed with previously mentioned immunoprecipitation lysis/wash buffer and subjected to Western blot analysis.

Cell death assessment

Cells were incubated for 20 min at 37°C with 10 µg/ml propidium iodide (Invitrogen) after the corresponding treatment. Cells were then washed with PBS and fixed for 10 min with 4% PFA as previously described (Lecoeur, 2002).

Immunocytochemistry

Cells were fixed for 10 min with 4% PFA and blocked with 5% normal goat serum (NGS; Sigma-Aldrich) with 0.1% Triton X-100 in PBS for 1 h at 20–26°C. Then, cells were incubated for 1 h at 20–26°C with antibodies for Olig2 (1:500; EMD Millipore), NG2 (1:200; EMD Millipore), MBP (1:500; Serotec), Ki67 (1:200; Vector Laboratories), or O4 (1:1,000; R&D Systems) in blocking solution. Upon primary antibody washes, fluorescently labeled secondary antibodies (1:500; Alexa Fluor [AF] 488 and AF568; Invitrogen) diluted at 1:500 in 5% NGS with 0.1% Triton X-100 were incubated for 1 h at 20–26°C. Nuclei were stained with 2 µg/ml Hoechst (Sigma-Aldrich) for 5 min, and two washes with PBS were performed before mounting the coverslips with Fluoromount G (SouthernBiotech).

Focal demyelination

Bilateral focal demyelination lesions were induced in the CCP of 2–3-mo-old female Sprague-Dawley rats in compliance with United Kingdom Home Office regulations (project license 70/7715). This involved stereotactic injections of 4 µl of 0.01% ethidium bromide (vol/vol) into the CCP. Animals were then perfused with 4% PFA at 5, 14, and 21 dpl. Once perfused, the removed brains were kept in 20% sucrose and embedded in optimal cutting temperature compound (Taab). Sections were cut to 12 µm and frozen at −80°C until further analysis.

Immunohistochemistry

12-µm sections were dried for 1 h at 20–26°C and washed with PBS before antigen retrieval. Antigen retrieval was performed by incubating the sections for 10 min at 75°C with preboiled 1× citrate buffer, pH 6.0, and antigen retriever (Dako). Then, slides were incubated for 6 h at 20–26°C with 5% normal donkey serum with 0.1% Triton X-100 and anti-Olig2 antibodies (1:200; R&D Systems). Slides were then incubated overnight at 4°C with antibodies against APC (1:200; EMD Millipore) and VDR (1:100; Santa Cruz Biotechnology, Inc.) in blocking solution. The remaining primary antibodies were washed away, and sections were incubated for 2 h at 20–26°C with 1:500 AF-conjugated secondary antibodies (1:300 donkey AF488 anti-goat, 1:500 donkey AF568 anti-rabbit, and 1:500 donkey AF647 anti-mouse [Invitrogen]) in 5% normal donkey serum with 0.1% Triton X-100. Nuclei were stained with 1 µg/ml Hoechst for 5 min, and slides were mounted after washes with Fluoromount G.

Organotypic cerebellar slices

Cerebellar slice cultures were prepared as previously described (Birgbauer et al., 2004). In brief, P9 rat cerebellum was isolated, and 300-µm sections were obtained using a tissue chopper (McIlwain). Slices were then incubated at 37°C with 5% CO_2 in organotypic slice medium composed of 50% HBSS (Gibco), 25% heat-inactivated horse serum (Gibco), 25% basal Eagle medium (Gibco), 5 mg/ml glucose, 1× glutamax (Gibco), and 1× Mycozap Plus-PR (Lonza). After 1 wk in culture, slices were demyelinated with 0.5 mg/ml lysolecithin (Sigma-Aldrich) for 16 h, and then medium was replaced with medium with the corresponding treatment. Treatment was replaced every other day, and slices were collected at 6 and 8 dpl and fixed with 4% PFA for 1 h. Then, slices were stored in 1× PBS at −20°C for immunostaining. In the case of myelination experiments, medium was replaced at 8 DIV with medium with the corresponding treatments, and no lysolecithin was added. For immunostaining, slices were blocked for 1 h with 10% NGS and 0.5% Triton X-100 in agitation and incubated overnight with antibodies against MBP (1:500; Serotec) and NFH (1:500; Abcam) in blocking solution. Slices were washed three times with 0.1% PBS and Triton X-100, and then incubated with secondary antibodies (1:300; AF488 and AF568; Invitrogen) for 2 h at 20–26°C. The secondary antibodies were removed by washing with 0.1% PBS and Triton X-100 and then Hoechst (1 µg/ml final concentration) was used for nuclei staining. Slices were mounted with Fluoromount G onto poly-ᴅ-lysine slides and covered with a 20-mm coverslip (VWR).

MS tissue samples and immunohistochemistry

MS patient brain samples were obtained from the UK MS Tissue Bank (Table S1). Control brain samples from individuals without evident neurological disease were also obtained from the same source. Tissues were collected with the donor's fully informed consent after ethical approval. Fixed frozen MS sections were hydrated in PBS and microwaved in antigen retrieval solution (Vector Laboratories) according to the manufacturer's protocol. Sections were preincubated in blocking buffer containing 10% NGS and 0.1% Triton X-100 in PBS for 1 h. Primary antibodies were incubated overnight at 4°C: GFAP (1:100; EMD

Millipore), Olig1 (1:50; R&D Systems), MOG (1:100; a gift from C. Linington, University of Glasgow, Glasgow, Scotland, UK), NeuN (1:50; EMD Millipore), MHC-II (1:50; Dako), Sox10 (1:50; R&D Systems), and VDR (1:100; Santa Cruz Biotechnology, Inc.). Primary antibodies were extensively washed with 0.1% PBS and Triton X-100 and incubated with appropriated secondary antibodies. Quantification of VDR+ cells was performed on high magnification fluorescent images of studied regions of interest using ImageJ version 1.44 software (National Institutes of Health) in at least three serial MS sections 100 µm apart from five MS and five control cases (Fig. 3 A). 6–10 pictures were taken for each MS region of interest, including active chronic lesions, PPWM, as well as NAWM from nonneurological controls. The number of immunopositive cells per square millimeter was calculated.

Quantification

For in vitro data obtained with OPC cultures, five randomly chosen areas of the coverslip were imaged per condition with the 20× objective (NA 0.30; Ph 1), or 40× (NA 0.50; Ph 1) for Duolink, using a fluorescence microscope (AxioVision Observer A1; Carl Zeiss) with a camera (Axio-Cam HRC; Carl Zeiss), and counting was done manually using the cell counter plugin in ImageJ. Organotypic cerebellar slices and in vivo CCP demyelination lesions were imaged using a confocal (SP5; Leica) and Advanced Fluorescence software, version 2.7.3.9723 (Leica). In the case of cerebellar slices, four independent slices were analyzed per condition and per experiment. Five images of randomly chosen areas of each slice were imaged using the 40× objective (NA 1.25) with 1.5× digital zoom, 1,024 × 1,024 resolution, and 1.75–2-µm thickness stacks. For analysis, a macro was created in ImageJ that measured the MBP–NFH colocalization area and the total NFH area. For CCP lesion images, the whole lesion of three sections was imaged per animal with the 20× objective (NA 0.70), 1,024 × 1,024 resolution, and 1.5–2-µm stacks. Using ImageJ software, the lesion area was delineated and measured, and the number of different cell types within the lesion was counted manually with the cell counter plugin. All the images were acquired at room temperature.

Statistics

Statistical analysis was performed using Prism 5.0 (GraphPad Software) and SPSS Statistics 20.0 (IBM). Mean ± SEM are shown in all the graphs. Agonist and antagonist treatments were analyzed by a one-way analysis of variance (ANOVA) followed by a Dunnett's post-hoc test, and VDR characterization in CCP lesions was analyzed by a one-way ANOVA followed by a Bonferroni post-hoc test or a Kruskal–Wallis test in cases of lack of normality (assessed using a Shapiro–Wilk test). siRNA experiments and charcoal treatment effect in MGCs and OPCs were analyzed using a bilateral unpaired Student's t test or Mann–Whitney U test in cases of lack of normality. Organotypic cerebellar slice experiments were analyzed by a two-way ANOVA followed by a Dunnett's post-hoc test. MS lesion VDR staining was analyzed using a one-way ANOVA with Bonferroni post-hoc tests.

Online supplemental material

Fig. S1 shows the effect of blocking VDR with the antagonist ZK159222 in the presence or absence of 9cRA, an RXR agonist. Fig. S2 shows the absence of effect of vitamin D in OPCs derived from MGCs exposed to normal serum in proliferation and differentiation. Table S1 provides the clinical data of the MS patients and matching controls used for this study. Table S2 shows the two independent measurements of vitamin D performed in the serum before and after charcoal treatment. Online supplemental material is available at http://www.jcb.org/cgi/content/full/jcb.201505119/DC1. Additional data are available in the JCB DataViewer at http://dx.doi.org/10.1083/jcb.201505119.dv.

References

Ascherio, A. 2013. Environmental factors in multiple sclerosis. *Expert Rev. Neurother.* 13:3–9. http://dx.doi.org/10.1586/14737175.2013.865866

Ascherio, A., K.L. Munger, and J.D. Lünemann. 2012. The initiation and prevention of multiple sclerosis. *Nat. Rev. Neurol.* 8:602–612. http://dx.doi.org/10.1038/nrneurol.2012.198

Baas, D., K. Prüfer, M.E. Ittel, S. Kuchler-Bopp, G. Labourdette, L.L. Sarlière, and P. Brachet. 2000. Rat oligodendrocytes express the vitamin D(3) receptor and respond to 1,25-dihydroxyvitamin D(3). *Glia.* 31:59–68. http://dx.doi.org/10.1002/(SICI)1098-1136(200007)31:1<59::AID-GLIA60>3.0.CO;2-Y

Birgbauer, E., T.S. Rao, and M. Webb. 2004. Lysolecithin induces demyelination in vitro in a cerebellar slice culture system. *J. Neurosci. Res.* 78:157–166. http://dx.doi.org/10.1002/jnr.20248

Bruce, S.J., B. Rochat, A. Béguin, B. Pesse, I. Guessous, O. Boulat, and H. Henry. 2013. Analysis and quantification of vitamin D metabolites in serum by ultra-performance liquid chromatography coupled to tandem mass spectrometry and high-resolution mass spectrometry—a method comparison and validation. *Rapid Commun. Mass Spectrom.* 27:200–206. http://dx.doi.org/10.1002/rcm.6439

Burton, J.M., and F.E. Costello. 2015. Vitamin D in multiple sclerosis and central nervous system demyelinating disease—a review. *J. Neuroophthalmol.* 35:194–200. http://dx.doi.org/10.1097/WNO.0000000000000256

Cantorna, M.T., C.E. Hayes, and H.F. DeLuca. 1996. 1,25-Dihydroxyvitamin D3 reversibly blocks the progression of relapsing encephalomyelitis, a model of multiple sclerosis. *Proc. Natl. Acad. Sci. USA.* 93:7861–7864. http://dx.doi.org/10.1073/pnas.93.15.7861

Casaccia-Bonnefil, P., and A. Liu. 2003. Relationship between cell cycle molecules and onset of oligodendrocyte differentiation. *J. Neurosci. Res.* 72:1–11. http://dx.doi.org/10.1002/jnr.10565

Chabas, J.F., D. Stephan, T. Marqueste, S. Garcia, M.N. Lavaut, C. Nguyen, R. Legre, M. Khrestchatisky, P. Decherchi, and F. Féron. 2013. Cholecalciferol (vitamin D3) improves myelination and recovery after nerve injury. *PLoS One.* 8:e65034. http://dx.doi.org/10.1371/journal.pone.0065034

de Lera, A.R., W. Bourguet, L. Altucci, and H. Gronemeyer. 2007. Design of selective nuclear receptor modulators: RAR and RXR as a case study. *Nat. Rev. Drug Discov.* 6:811–820. http://dx.doi.org/10.1038/nrd2398

Eyles, D.W., S. Smith, R. Kinobe, M. Hewison, and J.J. McGrath. 2005. Distribution of the vitamin D receptor and 1 α-hydroxylase in human brain. *J. Chem. Neuroanat.* 29:21–30. http://dx.doi.org/10.1016/j.jchemneu.2004.08.006

Franklin, R.J.M., and C. Ffrench-Constant. 2008. Remyelination in the CNS: from biology to therapy. *Nat. Rev. Neurosci.* 9:839–855. http://dx.doi.org/10.1038/nrn2480

Garcion, E., L. Sindji, C. Montero-Menei, C. Andre, P. Brachet, and F. Darcy. 1998. Expression of inducible nitric oxide synthase during rat brain inflammation: regulation by 1,25-dihydroxyvitamin D3. *Glia.* 22:282–294. http://dx.doi.org/10.1002/(SICI)1098-1136(199803)22:3<282::AID-GLIA7>3.0.CO;2-7

Garcion, E., L. Sindji, S. Nataf, P. Brachet, F. Darcy, and C.N. Montero-Menei. 2003. Treatment of experimental autoimmune encephalomyelitis in rat by

1,25-dihydroxyvitamin D3 leads to early effects within the central nervous system. *Acta Neuropathol.* 105:438–448.

Goldschmidt, T., J. Antel, F.B. König, W. Brück, and T. Kuhlmann. 2009. Remyelination capacity of the MS brain decreases with disease chronicity. *Neurology.* 72:1914–1921. http://dx.doi.org/10.1212/WNL.0b013e3181a8260a

Goudarzvand, M., M. Javan, J. Mirnajafi-Zadeh, S. Mozafari, and T. Tiraihi. 2010. Vitamins E and D3 attenuate demyelination and potentiate remyelination processes of hippocampal formation of rats following local injection of ethidium bromide. *Cell. Mol. Neurobiol.* 30:289–299. http://dx.doi.org/10.1007/s10571-009-9451-x

Herdick, M., A. Steinmeyer, and C. Carlberg. 2000. Antagonistic action of a 25-carboxylic ester analogue of 1α, 25-dihydroxyvitamin D3 is mediated by a lack of ligand-induced vitamin D receptor interaction with coactivators. *J. Biol. Chem.* 275:16506–16512. http://dx.doi.org/10.1074/jbc.M910000199

Huang, J.K., A.A. Jarjour, B. Nait Oumesmar, C. Kerninon, A. Williams, W. Krezel, H. Kagechika, J. Bauer, C. Zhao, A. Baron-Van Evercooren, et al. 2011. Retinoid X receptor gamma signaling accelerates CNS remyelination. *Nat. Neurosci.* 14:45–53. http://dx.doi.org/10.1038/nn.2702

Jarjour, A.A., H. Zhang, N. Bauer, C. Ffrench-Constant, and A. Williams. 2012. In vitro modeling of central nervous system myelination and remyelination. *Glia.* 60:1–12. http://dx.doi.org/10.1002/glia.21231

Kotter, M.R., W.W. Li, C. Zhao, and R.J.M. Franklin. 2006. Myelin impairs CNS remyelination by inhibiting oligodendrocyte precursor cell differentiation. *J. Neurosci.* 26:328–332. http://dx.doi.org/10.1523/JNEUROSCI.2615-05.2006

Kotter, M.R., C. Stadelmann, and H.P. Hartung. 2011. Enhancing remyelination in disease—can we wrap it up?. *Brain.* 134:1882–1900. http://dx.doi.org/10.1093/brain/awr014

Kuhlmann, T., V. Miron, Q. Cui, C. Wegner, J. Antel, and W. Brück. 2008. Differentiation block of oligodendroglial progenitor cells as a cause for remyelination failure in chronic multiple sclerosis. *Brain.* 131:1749–1758. http://dx.doi.org/10.1093/brain/awn096

Lecoeur, H. 2002. Nuclear apoptosis detection by flow cytometry: influence of endogenous endonucleases. *Exp. Cell Res.* 277:1–14. http://dx.doi.org/10.1006/excr.2002.5537

Lemire, J.M., and D.C. Archer. 1991. 1,25-dihydroxyvitamin D3 prevents the in vivo induction of murine experimental autoimmune encephalomyelitis. *J. Clin. Invest.* 87:1103–1107. http://dx.doi.org/10.1172/JCI115072

Levine, J.M., and R. Reynolds. 1999. Activation and proliferation of endogenous oligodendrocyte precursor cells during ethidium bromide-induced demyelination. *Exp. Neurol.* 160:333–347. http://dx.doi.org/10.1006/exnr.1999.7224

Lucchinetti, C., W. Brück, J. Parisi, B. Scheithauer, M. Rodriguez, and H. Lassmann. 2000. Heterogeneity of multiple sclerosis lesions: implications for the pathogenesis of demyelination. *Ann. Neurol.* 47:707–717. http://dx.doi.org/10.1002/1531-8249(200006)47:6<707::AID-ANA3>3.0.CO;2-Q

Masoumi, A., B. Goldenson, S. Ghirmai, H. Avagyan, J. Zaghi, K. Abel, X. Zheng, A. Espinosa-Jeffrey, M. Mahanian, P.T. Liu, et al. 2009. 1α,25-dihydroxyvitamin D3 interacts with curcuminoids to stimulate amyloid-β clearance by macrophages of Alzheimer's disease patients. *J. Alzheimers Dis.* 17:703–717.

McCarthy, K.D., and J. de Vellis. 1980. Preparation of separate astroglial and oligodendroglial cell cultures from rat cerebral tissue. *J. Cell Biol.* 85:890–902. http://dx.doi.org/10.1083/jcb.85.3.890

McLeod, J.F., and N.E. Cooke. 1989. The vitamin D-binding protein, α-fetoprotein, albumin multigene family: detection of transcripts in multiple tissues. *J. Biol. Chem.* 264:21760–21769.

Miron, V.E., A. Boyd, J.-W. Zhao, T.J. Yuen, J.M. Ruckh, J.L. Shadrach, P. van Wijngaarden, A.J. Wagers, A. Williams, R.J.M. Franklin, and C. ffrench-Constant. 2013. M2 microglia and macrophages drive oligodendrocyte differentiation during CNS remyelination. *Nat. Neurosci.* 16:1211–1218. http://dx.doi.org/10.1038/nn.3469

Mokry, L.E., S. Ross, O.S. Ahmad, V. Forgetta, G.D. Smith, A. Leong, C.M.T. Greenwood, G. Thanassoulis, and J.B. Richards. 2015. Vitamin D and risk of multiple sclerosis: A Mendelian randomization study. *PLoS Med.* 12:e1001866. http://dx.doi.org/10.1371/journal.pmed.1001866

Montava, M., S. Garcia, J. Mancini, Y. Jammes, J. Courageot, J.-P. Lavieille, and F. Féron. 2015. Vitamin D3 potentiates myelination and recovery after facial nerve injury. *Eur. Arch. Otorhinolaryngol.* 272:2815–2823. http://dx.doi.org/10.1007/s00405-014-3305-y

Moyon, S., A.L. Dubessy, M.S. Aigrot, M. Trotter, J.K. Huang, L. Dauphinot, M.C. Potier, C. Kerninon, S. Melik Parsadaniantz, R.J.M. Franklin, and C. Lubetzki. 2015. Demyelination causes adult CNS progenitors to revert to an immature state and express immune cues that support their migration. *J. Neurosci.* 35:4–20. http://dx.doi.org/10.1523/JNEUROSCI.0849-14.2015

Munger, K.L., S.M. Zhang, E. O'Reilly, M.A. Hernán, M.J. Olek, W.C. Willett, and A. Ascherio. 2004. Vitamin D intake and incidence of multiple sclerosis. *Neurology.* 62:60–65. http://dx.doi.org/10.1212/01.WNL.0000101723.79681.38

Munger, K.L., L.I. Levin, B.W. Hollis, N.S. Howard, and A. Ascherio. 2006. Serum 25-hydroxyvitamin D levels and risk of multiple sclerosis. *JAMA.* 296:2832–2838. http://dx.doi.org/10.1001/jama.296.23.2832

Nataf, S., E. Garcion, F. Darcy, D. Chabannes, J.Y. Muller, and P. Brachet. 1996. 1,25 Dihydroxyvitamin D3 exerts regional effects in the central nervous system during experimental allergic encephalomyelitis. *J. Neuropathol. Exp. Neurol.* 55:904–914. http://dx.doi.org/10.1097/00005072-199608000-00006

Nystad, A.E., S. Wergeland, L. Aksnes, K.M. Myhr, L. Bø, and O. Torkildsen. 2014. Effect of high-dose 1.25 dihydroxyvitamin D3 on remyelination in the cuprizone model. *APMIS.* 122:1178–1186. http://dx.doi.org/10.1111/apm.12281

Pérez, E., W. Bourguet, H. Gronemeyer, and A.R. de Lera. 2012. Modulation of RXR function through ligand design. *Biochim. Biophys. Acta.* 1821:57–69. http://dx.doi.org/10.1016/j.bbalip.2011.04.003

Schmitz, A.A., S. Hackethal, A. Schulz, E. May, A. Steinmeyer, U. Zügel, and K. Asadullah. 2015. Sharing pharma compounds with academia: experiences with providing vitamin D receptor ligands. *Nat. Rev. Drug Discov.* 14:294–294. http://dx.doi.org/10.1038/nrd4008-c1

Shen, S., J. Sandoval, V.A. Swiss, J. Li, J. Dupree, R.J.M. Franklin, and P. Casaccia-Bonnefil. 2008. Age-dependent epigenetic control of differentiation inhibitors is critical for remyelination efficiency. *Nat. Neurosci.* 11:1024–1034. http://dx.doi.org/10.1038/nn.2172

Shields, S., J. Gilson, W. Blakemore, and R. Franklin. 2000. Remyelination occurs as extensively but more slowly in old rats compared to young rats following fliotoxin-induced CNS demyelination. *Glia.* 29:102. http://dx.doi.org/10.1002/(SICI)1098-1136(20000101)29:1<102::AID-GLIA12>3.0.CO;2-1

Shirazi, H.A., J. Rasouli, B. Ciric, A. Rostami, and G.-X. Zhang. 2015. 1,25-Dihydroxyvitamin D3 enhances neural stem cell proliferation and oligodendrocyte differentiation. *Exp. Mol. Pathol.* 98:240–245. http://dx.doi.org/10.1016/j.yexmp.2015.02.004

Sim, F.J., C. Zhao, J. Penderis, and R.J.M. Franklin. 2002. The age-related decrease in CNS remyelination efficiency is attributable to an impairment of both oligodendrocyte progenitor recruitment and differentiation. *J. Neurosci.* 22:2451–2459.

Smolders, J., K.G. Schuurman, M.E. van Strien, J. Melief, D. Hendrickx, E.M. Hol, C. van Eden, S. Luchetti, and I. Huitinga. 2013. Expression of vitamin D receptor and metabolizing enzymes in multiple sclerosis-affected brain tissue. *J. Neuropathol. Exp. Neurol.* 72:91–105. http://dx.doi.org/10.1097/NEN.0b013e31827f4fcc

Soilu-Hänninen, M., L. Airas, I. Mononen, A. Heikkilä, M. Viljanen, and A. Hänninen. 2005. 25-Hydroxyvitamin D levels in serum at the onset of multiple sclerosis. *Mult. Scler.* 11:266–271. http://dx.doi.org/10.1191/1352458505ms1157oa

Soilu-Hänninen, M., M. Laaksonen, I. Laitinen, J.-P. Erälinna, E.-M. Lilius, and I. Mononen. 2008. A longitudinal study of serum 25-hydroxyvitamin D and intact parathyroid hormone levels indicate the importance of vitamin D and calcium homeostasis regulation in multiple sclerosis. *J. Neurol. Neurosurg. Psychiatry.* 79:152–157. http://dx.doi.org/10.1136/jnnp.2006.105320

van den Ouweland, J.M.W., A.M. Beijers, and H. van Daal. 2014. Overestimation of 25-hydroxyvitamin D3 by increased ionisation efficiency of 3-epi-25-hydroxyvitamin D3 in LC-MS/MS methods not separating both metabolites as determined by an LC-MS/MS method for separate quantification of 25-hydroxyvitamin D3, 3-epi-25-hydroxyvitamin D3 and 25-hydroxyvitamin D2 in human serum. *J. Chromatogr. B Analyt. Technol. Biomed. Life Sci.* 967:195–202. http://dx.doi.org/10.1016/j.jchromb.2014.07.021

Wergeland, S., Ø. Torkildsen, K.-M. Myhr, L. Aksnes, S.J. Mørk, and L. Bø. 2011. Dietary vitamin D3 supplements reduce demyelination in the cuprizone model. *PLoS One.* 6:e26262. http://dx.doi.org/10.1371/journal.pone.0026262

Wolswijk, G. 1998. Chronic stage multiple sclerosis lesions contain a relatively quiescent population of oligodendrocyte precursor cells. *J. Neurosci.* 18:601–609.

Woodruff, R.H., and R.J. Franklin. 1999. Demyelination and remyelination of the caudal cerebellar peduncle of adult rats following stereotaxic injections of lysolecithin, ethidium bromide, and complement/anti-galactocerebroside: a comparative study. *Glia.* 25:216–228. http://dx.doi.org/10.1002/(SICI)1098-1136(19990201)25:3<216::AID-GLIA2>3.0.CO;2-L

Woodruff, R.H., M. Fruttiger, W.D. Richardson, and R.J.M. Franklin. 2004. Platelet-derived growth factor regulates oligodendrocyte progenitor numbers in adult CNS and their response following CNS demyelination. *Mol. Cell. Neurosci.* 25:252–262. http://dx.doi.org/10.1016/j.mcn.2003.10.014

Zawadzka, M., L.E. Rivers, S.P.J. Fancy, C. Zhao, R. Tripathi, F. Jamen, K. Young, A. Goncharevich, H. Pohl, M. Rizzi, et al. 2010. CNS-resident glial progenitor/stem cells produce Schwann cells as well as oligodendrocytes during repair of CNS demyelination. *Cell Stem Cell.* 6:578–590. http://dx.doi.org/10.1016/j.stem.2010.04.002

Zhang, H., A.A. Jarjour, A. Boyd, and A. Williams. 2011. Central nervous system remyelination in culture—a tool for multiple sclerosis research. *Exp. Neurol.* 230:138–148. http://dx.doi.org/10.1016/j.expneurol.2011.04.009

Zhang, Y., K. Chen, S.A. Sloan, M.L. Bennett, A.R. Scholze, S. O'Keeffe, H.P. Phatnani, P. Guarnieri, C. Caneda, N. Ruderisch, et al. 2014. An RNA-sequencing transcriptome and splicing database of glia, neurons, and vascular cells of the cerebral cortex. *J. Neurosci.* 34:11929–11947. http://dx.doi.org/10.1523/JNEUROSCI.1860-14.2014